

Supplementary Information for

Structural Water in Amorphous Carbonate Minerals: Ab
Initio Molecular Dynamics Simulations of X-ray Pair
Distribution Experiments

*Micah P. Prange, Sebastian T. Mergelsberg, and Sebastien N. Kerisit**

Physical and Computational Sciences Directorate, Pacific Northwest National Laboratory,
Richland, Washington 99352, United States

Exchange-correlation (XC) functionals

XC functionals were evaluated by comparing calculated lattice parameters to experimental lattice parameters from the literature.

Table S1. Experimental and calculated lattice parameters of the three carbonate minerals (aragonite, calcite and monohydrocalcite) used as benchmarks in Figure 1. The calculated lattice parameters were obtained from constant-pressure energy minimizations.

Phase	Aragonite						Calcite				Monohydrocalcite				RMSD
XC	a (Å)	Δa (%)	b (Å)	Δb (%)	c (Å)	Δc (%)	a (Å)	Δa (%)	c (Å)	Δc (%)	a (Å)	Δa (%)	c (Å)	Δc (%)	
Expt. ^a	4.9616	--	7.9705	--	5.7394	0.0	4.988	--	17.061	--	10.5536	--	7.5446	--	--
PBE-G	4.9832	0.4	7.9470	-0.3	5.7388	0.0	5.027	0.8	17.008	-0.3	10.5079	-0.4	7.5485	0.1	0.408
revPBE-G	5.0189	1.2	7.9880	0.2	5.7619	0.4	5.060	1.4	17.100	0.2	10.5467	-0.1	7.5821	0.5	0.747
PBE	5.0009	0.8	8.0071	0.5	5.7896	0.9	5.041	1.1	17.180	0.7	10.6143	0.6	7.6280	1.1	0.827
PBEsol	4.9422	-0.4	7.9137	-0.7	5.6441	-1.7	4.989	0.0	16.843	-1.3	10.4028	-1.4	7.4855	-0.8	1.049
RPBE-G	5.0408	1.6	8.0343	0.8	5.8187	1.4	5.081	1.9	17.200	0.8	10.6195	0.6	7.6467	1.4	1.278
PBEsol-G	4.9248	-0.7	7.8766	-1.2	5.5873	-2.6	4.983	-0.1	16.638	-2.5	10.3287	-2.1	7.4251	-1.6	1.780
revPBE	5.0592	2.0	8.0839	1.4	5.9200	3.1	5.081	1.9	17.533	2.8	10.8052	2.4	7.7621	2.9	2.419
RPBE	5.0750	2.3	8.1146	1.8	5.9609	3.9	5.095	2.1	17.662	3.5	10.8655	3.0	7.8015	3.4	2.945

^aAragonite: A. Dal Negro and L. Ungaretti, *American Mineralogist*, 1971, **56**, 768-772; calcite: S.A. Markgraf and R.J. Reeder, *American Mineralogist*, 1985, **70**, 590-600; monohydrocalcite: E. Effenberger, *Monatshefte für Chemie*, 1981, **112**, 899-909.

Dynamics of the melted systems

The dynamics of the melted systems (amorphous magnesium/calcium/strontium carbonate (AMC/ACC/ASC), $\text{Mg/Ca/SrCO}_3 \cdot n\text{H}_2\text{O}$ with $n = 0, 0.5, 1, 1.5$ or 2) were characterized through analysis of the residence time of O atoms in the first coordination shell of Mg, Ca, or Sr and of the mean square displacement (MSD) of Mg, Ca, Sr, C, and O atoms.

The residence time of an oxygen atom in the first coordination shell of a divalent cation was calculated from the residence-time correlation functions, which is defined as

$$\langle R(t) \rangle = \left\langle \frac{1}{N_0} \sum_{i=1}^{N_t} \theta_i(0) \theta_i(t) \right\rangle \quad (1)$$

where N_t is the number of oxygen atoms in the first coordination shell of a divalent cation at time t and $\theta_i(t)$ is the Heaviside function, which is 1 if the i^{th} oxygen atom is in the first coordination shell at time t and 0 otherwise. To account for the timescale required for an oxygen atom to exchange between the first and second coordination shells, an oxygen atom was counted as having left the first coordination shell if it had done so for at least 0.5 ps. The residence time can be obtained by integration of $\langle R(t) \rangle$

$$\tau = \int_0^{\infty} \langle R(t) \rangle dt \quad (2)$$

If $\langle R(t) \rangle$ does not reach zero by the end of the simulation, τ can be obtained by fitting $\langle R(t) \rangle$ with an exponential function. Fig. S1 shows the residence time correlation functions computed from the AMC, ACC, and ASC melt simulations at the five hydration levels.

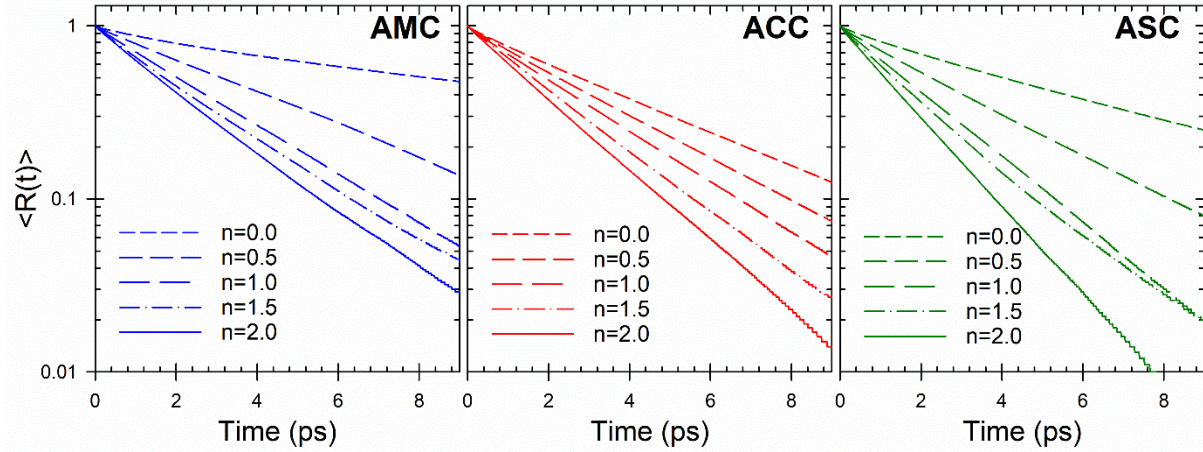


Figure S1. Divalent cation–oxygen residence time correlation functions computed from the AMC, ACC, and ASC melt simulations (1500 K) at five hydration levels ($n = 0, 0.5, 1$, and $1.5, 2$).

The time required to exchange half of the divalent cation first coordination shell (half-life value) at each hydration level is shown in Table S2. All half-life values are smaller than the configuration collection time (16 ps for the first configuration and 9 ps thereafter).

Table S2. Half-life values (in ps) of the divalent cation first coordination shell in the melted systems.

System	$n = 0$	$n = 0.5$	$n = 1$	$n = 1.5$	$n = 2$
AMC	7.8	3.2	2.1	1.9	1.7
ACC	2.9	2.4	2.0	1.7	1.5
ASC	4.3	2.4	1.6	1.5	1.2

The self-diffusion coefficients of Mg, Sr, Ca, C, and O were obtained from their mean square displacement (MSD_i)

$$\text{MSD}_i = \langle |r_i(t) - r_i(0)|^2 \rangle \quad (3)$$

where $r_i(t)$ is the position of atom i at time t . A configuration was recorded every 12.5 fs, and the MSDs were calculated for a correlation period of 12 ps. The diffusion coefficient of atom i , D_i , is given by the Einstein relation

$$D_i = \frac{MSD_i}{2nt} \quad (4)$$

where n is the number of dimensions in which the diffusion coefficient is considered. The first 2 ps of the MSD were ignored to avoid including the ballistic regime in the determination of D_i . Fig. S2 shows the MSD_i computed for $i = \text{Mg, Ca, Sr, C, or O}$ in the melted systems.

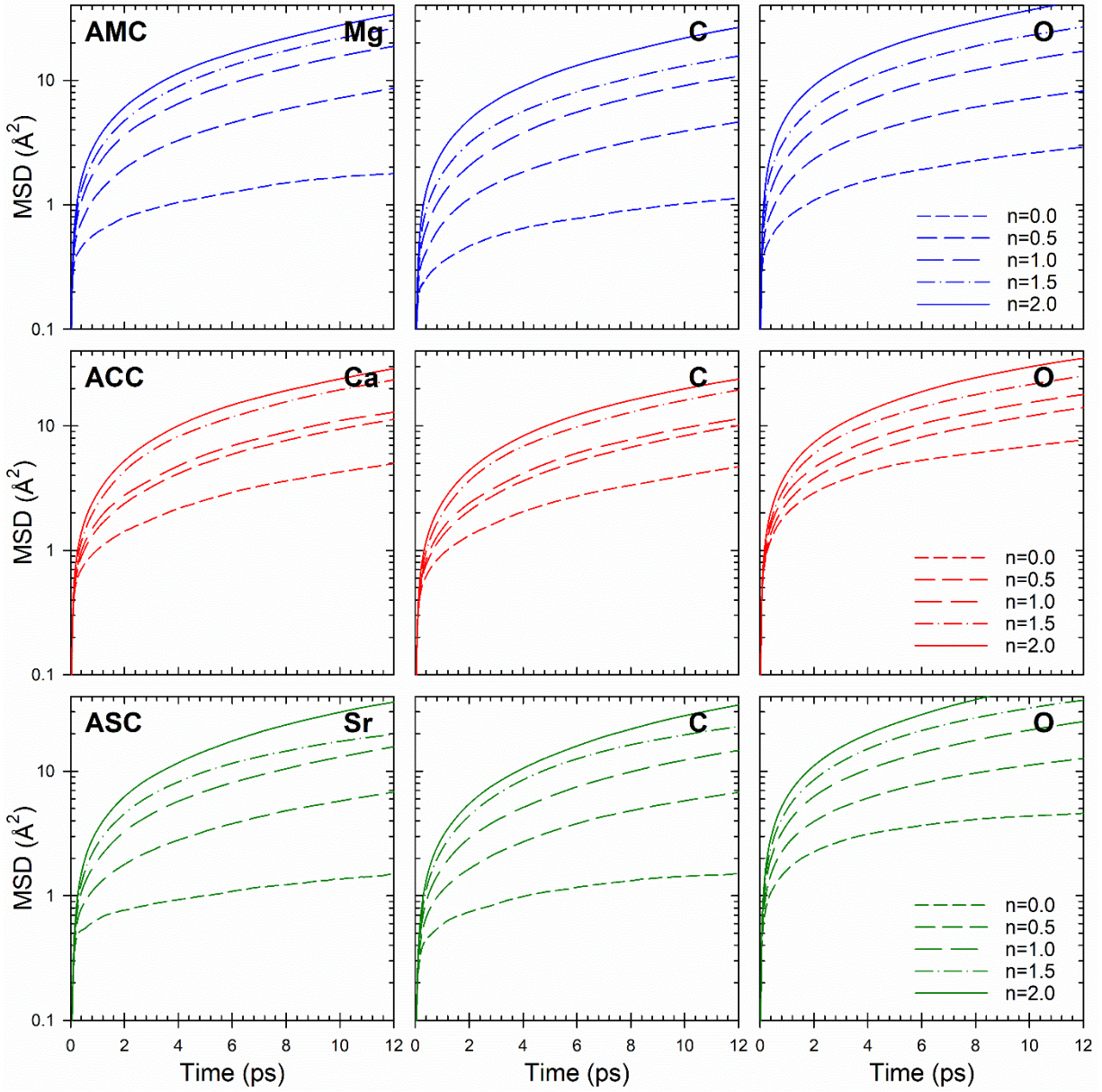


Figure S2. Mg, Ca, Sr, C, and O mean square displacements in the melt simulations.

The resulting D_i values are tabulated in Table S3. For comparison, the diffusion coefficients of liquid water and olive oil at room temperature are approximately 2.5×10^{-9} and $0.065 \times 10^{-9} \text{ m}^2 \text{ s}^{-1}$.

Table S3. Diffusion coefficients ($10^{-9} \text{ m}^2/\text{s}$) of Mg, Ca, Sr, C, and O in the melted systems.

Element	$n = 0$	$n = 0.5$	$n = 1$	$n = 1.5$	$n = 2$
AMC–Mg	0.17	1.10	2.53	3.57	4.56
AMC–C	0.11	0.58	1.46	2.07	3.59
AMC–O	0.29	0.96	2.17	3.45	5.75
ACC–Ca	0.59	1.48	1.71	3.15	3.87
ACC–C	0.55	1.32	1.51	2.59	3.22
ACC–O	0.75	1.68	2.19	3.13	4.60
ASC–Sr	0.12	0.83	2.05	2.54	5.00
ASC–C	0.13	0.85	1.99	3.08	4.80
ASC–O	0.36	1.43	3.09	4.76	7.49

Density estimates from NPT simulations

An example of the variation of the instantaneous density during a 12-ps NPT AIMD simulation of ACC ($n=1$) and its Gaussian distribution are shown in Fig. S3.

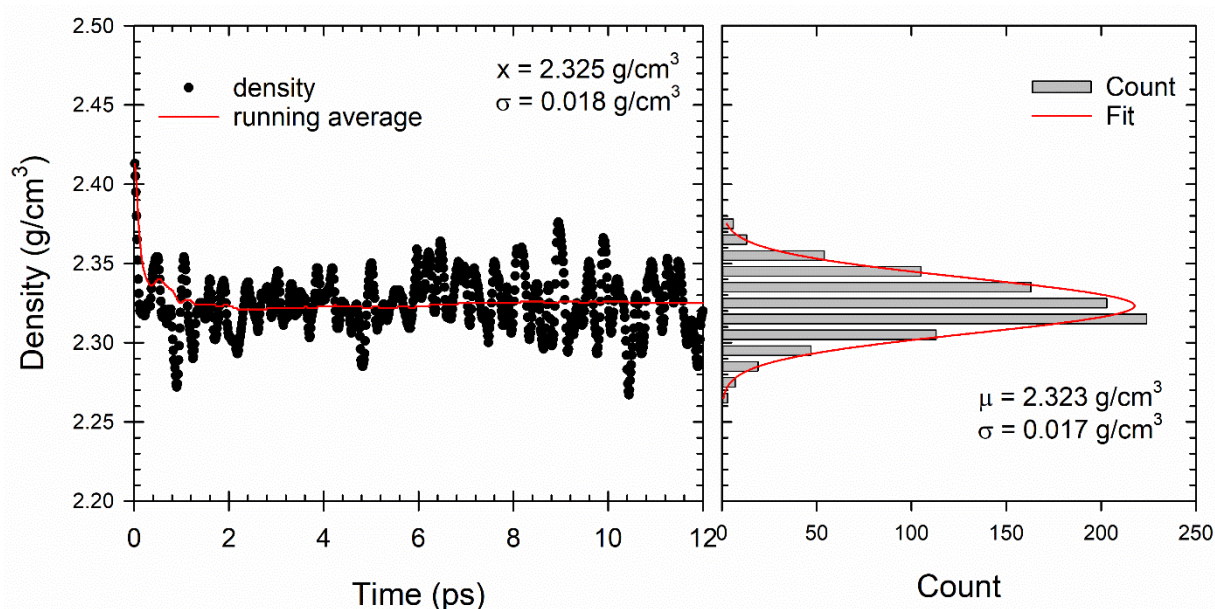


Figure S3. (left) Variation and running average of the instantaneous density during an NPT AIMD simulation of ACC ($n=1$) (mean density and standard deviation of instantaneous density are shown in the panel). (right) Histogram of the instantaneous density (the first three data points were omitted) and Gaussian fit (mean density and standard deviation from the Gaussian fit are shown in the panel).

Snapshots of ab initio molecular dynamics (AIMD) simulations

Snapshots of the NPT AIMD simulations are shown in Figs. S4 (amorphous magnesium carbonate), S5 (amorphous calcium carbonate), and S6 (amorphous strontium carbonate). Each snapshot shows a central divalent cation and all cations, (bi)carbonate anions, hydroxide anions, and water molecules with their central atom (C for (bi)carbonate and O for hydroxide and water) within 5 Å of the central divalent cation. Fig. S7 shows another view of amorphous magnesium carbonate highlighting three cations bridged by a carbonate group.

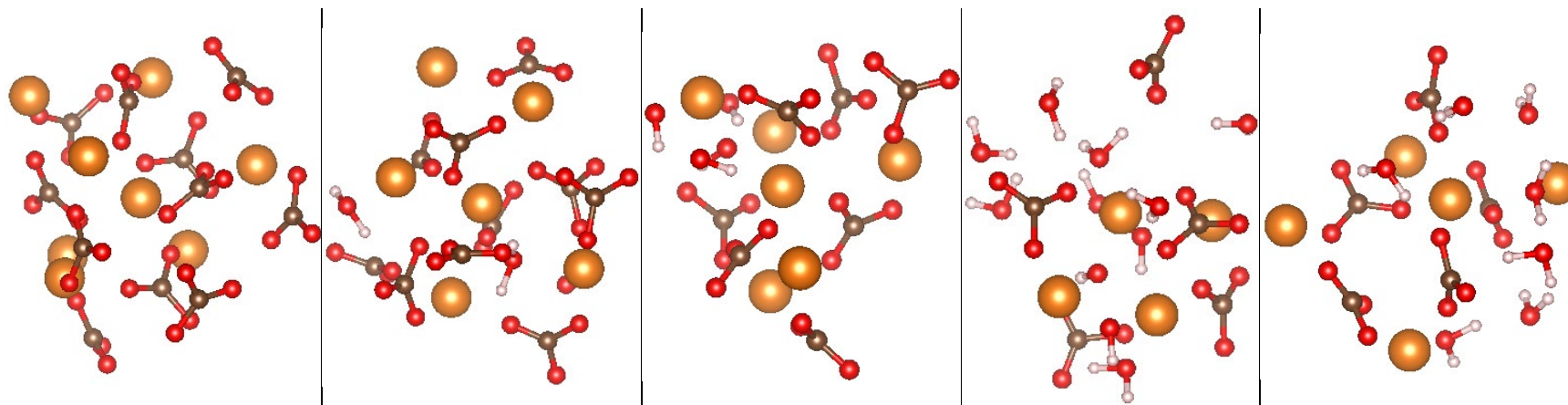


Figure S4. Snapshots of the AMC ($\text{MgCO}_3 \cdot n\text{H}_2\text{O}$) AIMD simulations with, from left to right, $n = 0, 0.5, 1.0, 1.5$, and 2 .

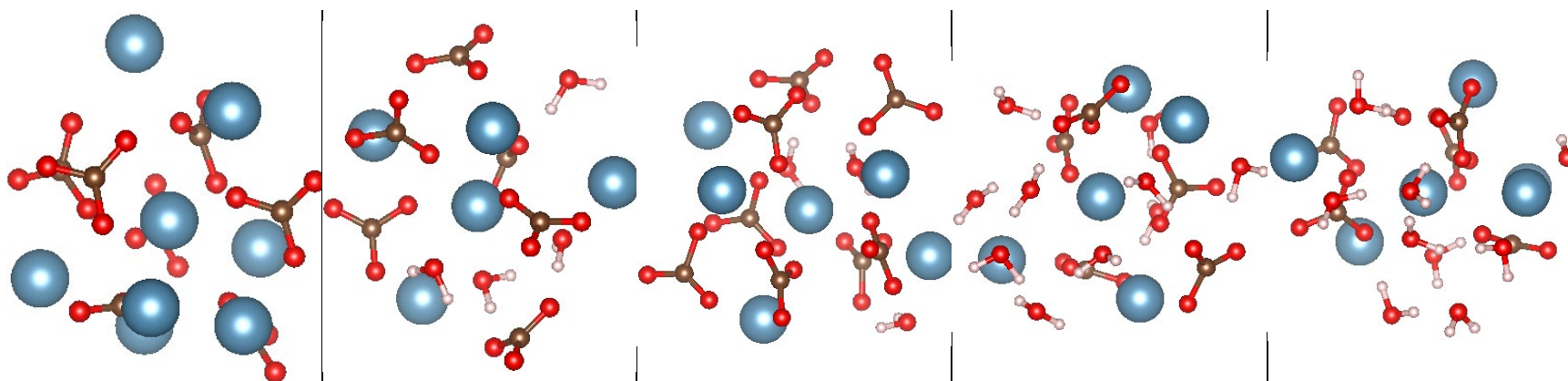


Figure S5. Snapshots of the ACC ($\text{CaCO}_3 \cdot n\text{H}_2\text{O}$) AIMD simulations with, from left to right, $n = 0, 0.5, 1.0, 1.5$, and 2 .

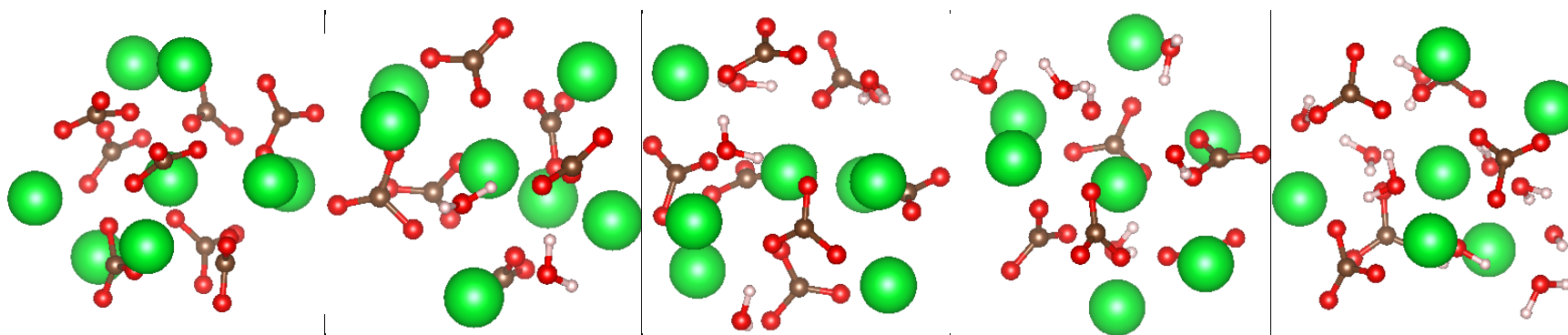


Figure S6. Snapshots of the ASC ($\text{SrCO}_3 \cdot n\text{H}_2\text{O}$) AIMD simulations with, from left to right, $n = 0, 0.5, 1.0, 1.5$, and 2 .

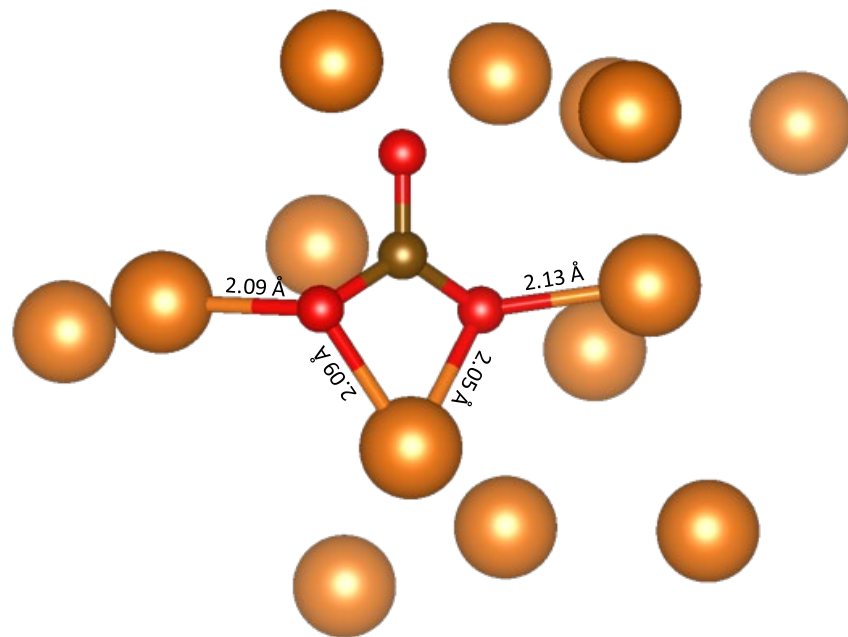


Figure S7. Motif occurring in the anhydrous AMC simulations in which a CO_3^{2-} anion in bidentate conformation of one Mg^{2+} cation bridges two other axial Mg^{2+} ions.

Radial distribution functions

Radial distribution functions $g(r)$ for the amorphous carbonate models are shown in Figs. S8 and S9.

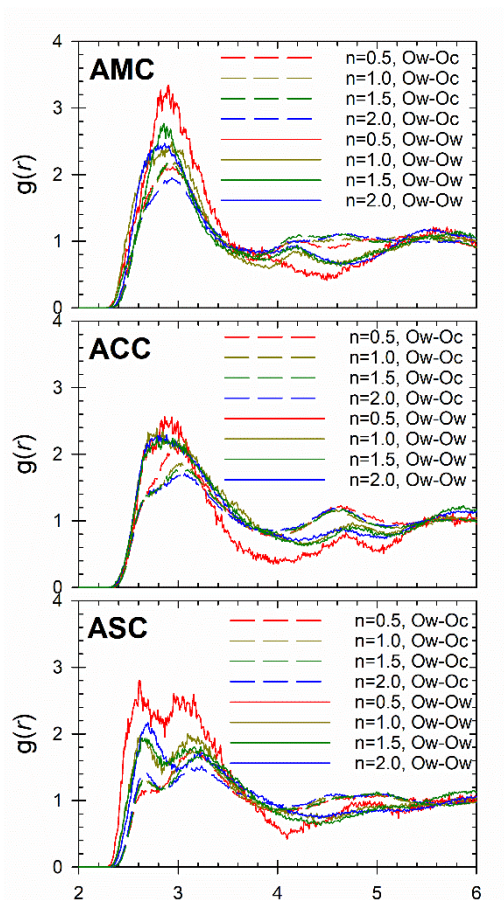


Figure S8. Water/hydroxide oxygen-carbonate/bicarbonate oxygen (Ow-Oc, dashed lines) and water/hydroxide oxygen-water/hydroxide oxygen (Ow-Ow, solid lines) radial distribution functions for various hydration levels for AMC (top), ACC (middle), and ASC (bottom).

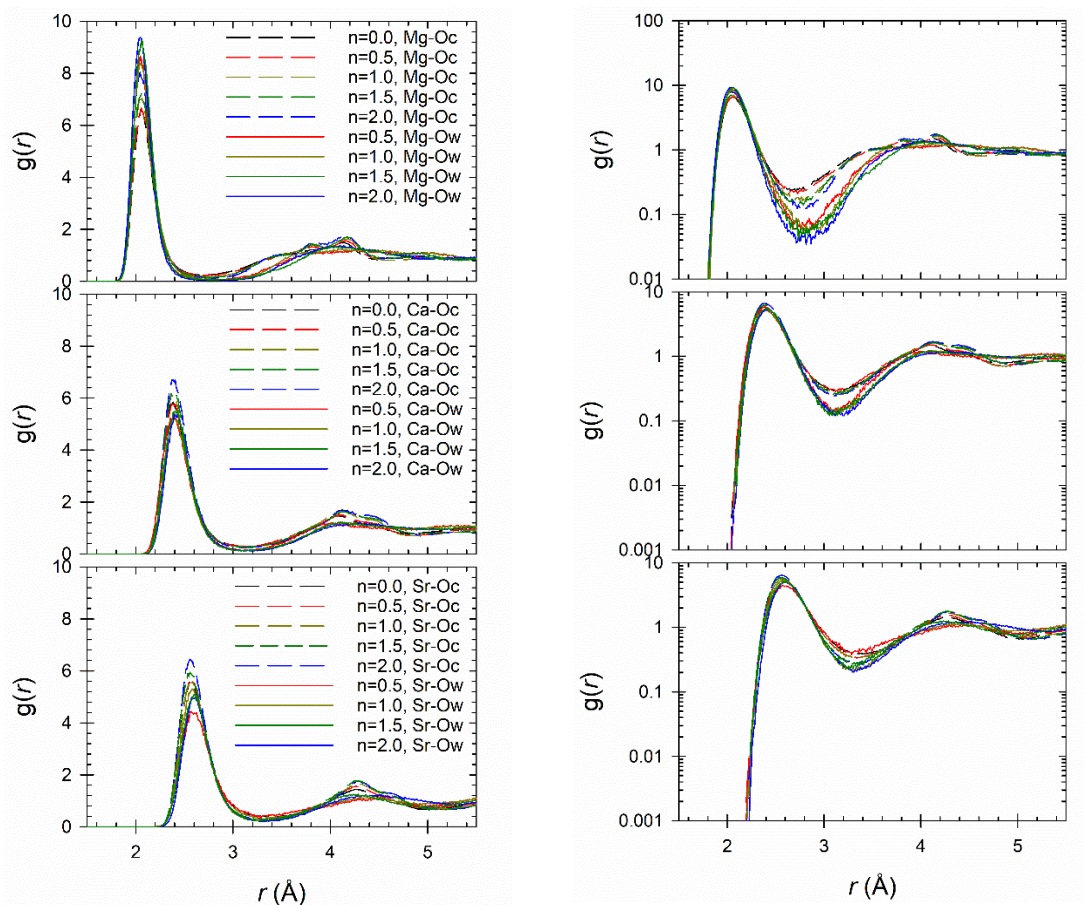


Figure S9. Metal-carbonate/bicarbonate oxygen (M-Oc, dashed lines) and metal-water/hydroxide oxygen (M-Ow, solid lines) radial distribution functions for various hydration levels for AMC (top), ACC (middle), and ASC (bottom) on linear-linear (left) and log-linear (right) scales.